**SUPPORTING MATERIAL**

# Giant unilamellar vesicles formed by hybrid films of lipids and agarose display altered mechanical properties

Rafael B. Lira[1,2], Rumiana Dimova[2], Karin A. Riske[1]

[1] Departamento de Biofísica, Universidade Federal de São Paulo, São Paulo, Brazil.

[2] Department of Theory and Bio-Systems, Max Planck Institute of Colloids and Interfaces, Potsdam, Germany.

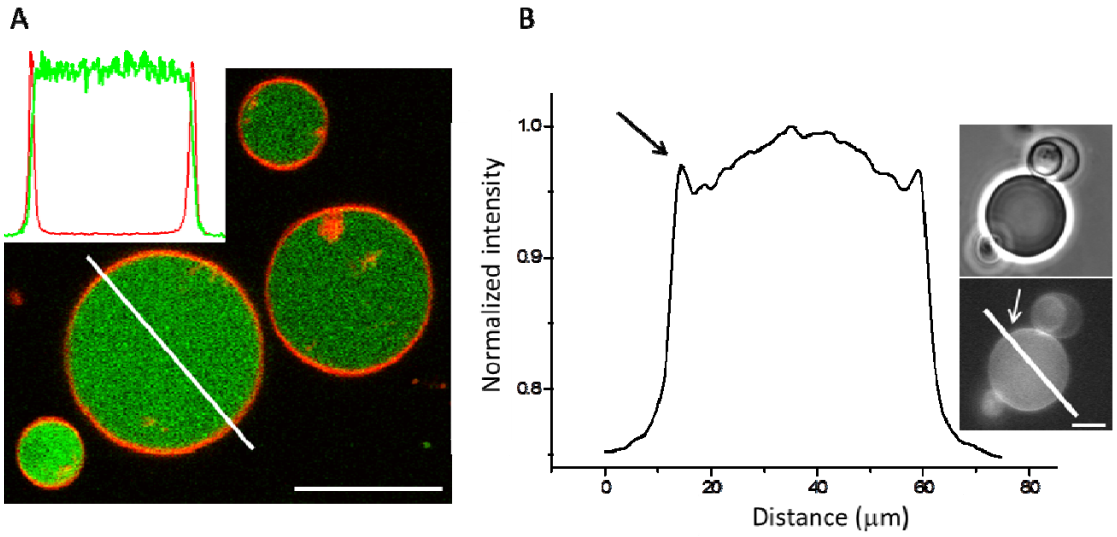


**Figure S1.** GUVs grown on hybrid films of fluorescent agarose and lipids. A: confocal microscopy image of typical agarose-GUVs (POPC:POPG 8:2) encapsulating fluorescent agarose (green). Lipid membrane contains 0.5 mol% DPPE-Rh (red). Fluorescence intensity profiles of both agarose (green curve) and membrane probe (red curve) measured along the white line is shown in the inset. B: Fluorescence intensity profile of fluorescent agarose measured along the white line across the agarose-GUV grown (epifluorescence microscopy) and dispersed in sugar containing 100 mM NaCl shown in the inset (bottom). The arrows point to the high fluorescence intensity at the vesicle surface, indicating agarose binding to the membrane. The inset also shows a phase contrast image of the same vesicle (up). Bars: 20 μm.

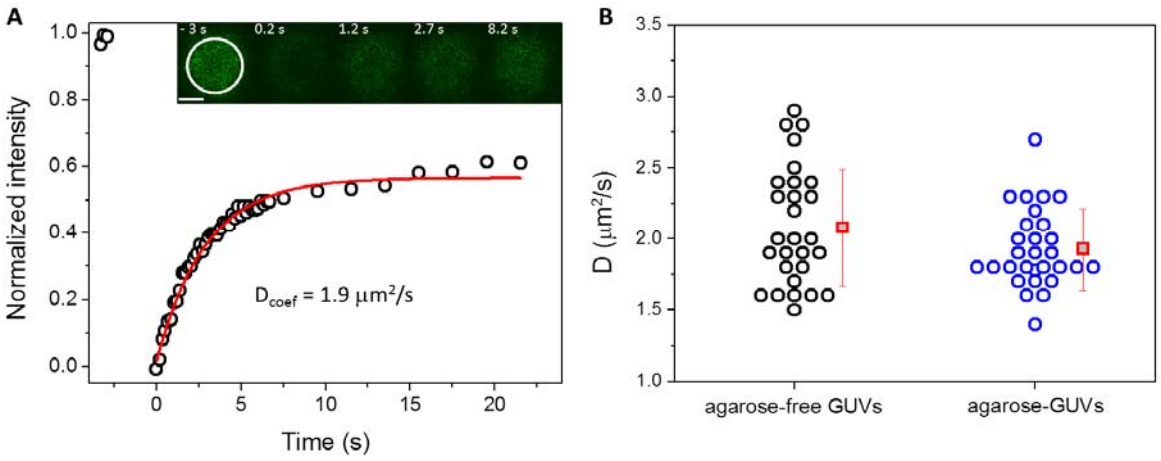


**Figure S2.** Lipid mobility is not affected by the method of producing vesicles as probed by fluorescence recovery after photobleaching (FRAP). FRAP was performed either on the upper surface or at the vesicle equator of GUVs of POPC:POPG 8:2 with 0.5 mol% of head-labeled NBD-PE lipids immobilized in an agarose mesh (Lira *et al.*, unpublished results). A) One example for a FRAP measurement done on the vesicle surface. The inset shows an image sequence of FRAP on the pole of a GUV. The region of interest (ROI) of 10 µm diameter is shown as a white circle on the first image. Bar: 5 µm. Photobleaching was achieved via irradiation with 488 nm laser at high power (80% of maximal achieved power) for 1.3 s. Images were recorded at 162 ms time resolution for 40 s, enough to achieve stable recovery. The graph shows the fluorescence intensity inside the ROI normalized by the initial intensity (black circles), before photobleaching. The first data points are fluorescence intensity values before photobleaching. The value reached after fluorescence recovery is smaller than the initial value (because the recovery scales with the vesicle radius) and was not sensitive to the presence of encapsulated agarose. The corresponding best fit (exponential with a characteristic time $\tau$) is shown as red curve. The diffusion coefficient D was measured assuming a simple 2-dimensional diffusion using $D = 0.88r^2/4\tau$ , where $r$ is the effective ROI radius and $\tau$ the recovery time obtained by fitting of the data (red curve). In the case shown in A, D = 1.9 µm$^2$/s. D was measured for several GUVs (total of 28 agarose-free GUVs and 29 agarose-GUVs) and the results are shown in panel (B). Each data point corresponds to one vesicle. The mean values with standard deviation are also shown. There is no marked difference between D values measured on agarose-free and agarose-GUVs, indicating no hindered lipid diffusion due to the presence of encapsulated agarose. The mean D values obtained were 2.1 ± 0.4 and 1.9 ± 0.3 µm$^2$/s for agarose-free and agarose-GUVs, respectively.

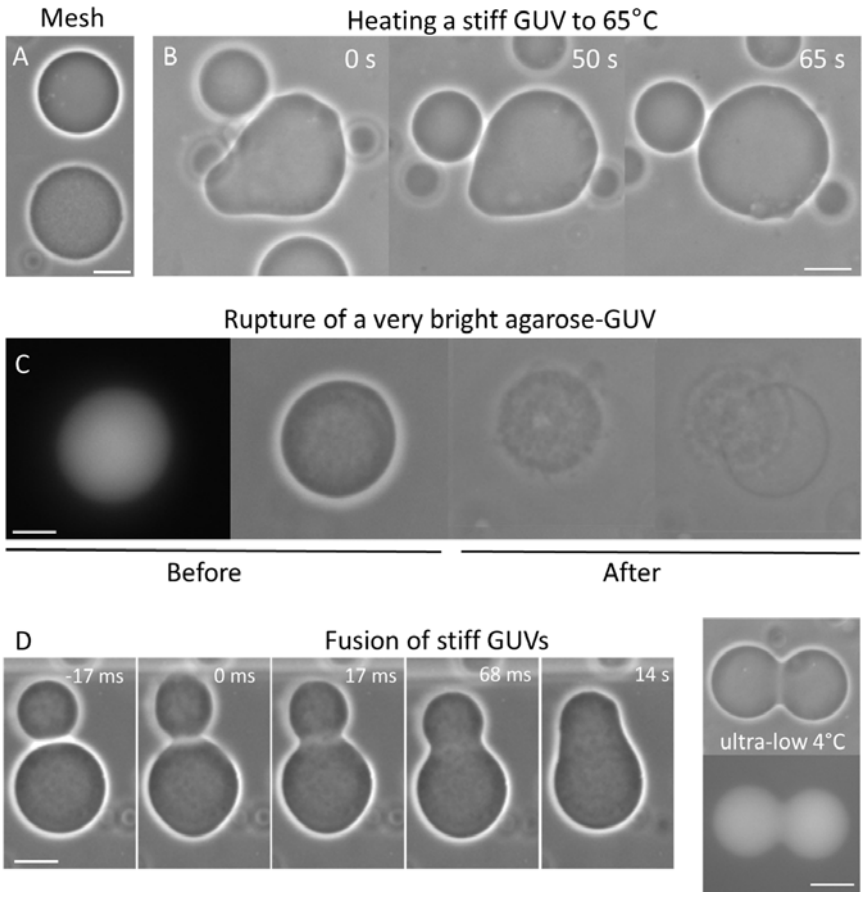


**Figure S3.** Morphological changes in agarose-GUVs. Panel A shows phase contrast images of one typical agarose-GUV encapsulating agarose at low or intermediate concentrations (above) and an agarose-GUV encapsulating a gel-like meshwork (below). B: Phase contrast sequence showing the effect of temperature on a stiff agarose-GUV. The first snapshot shows the GUV at room temperature; the GUV maintains faceted shape and the membrane hardly exhibits thermal fluctuations. The following images show the vesicle when the temperature is increased to 65°C, i.e., above agarose $T_m$ ~ 58°C when the polymer melts. The membrane starts to fluctuate only above the melting transition of agarose (last snapshot). C: An agarose-GUV formed on hybrid films of fluorescent agarose. This vesicle looks stiff, is strongly fluorescent (first image – fluorescence mode) and has a gel-like meshwork encapsulated (second image – phase contrast). Upon electroporation, the gel meshwork is expelled through a macropore and the membrane reseals forming a smaller GUV (last two images). D: Two stiff agarose-GUVs were found in close proximity and fused after electroporation (electrofusion). Although membranes are fused, their internal contents are not completely mixed and the fused GUV maintains a stable dumbbell shape, which would not be expected for a fluid vesicle encapsulating a completely fluid solution. Fusion without complete content mixing can also be observed when ultra-low gelling temperature agarose-GUVs are grown at 4°C, thus resulting in GUVs encapsulating gel state agarose (last snapshot). The polymer was fluorescently labeled and can be seen encapsulated on the final dumbbell-shaped GUV. Bars: 20 μm.

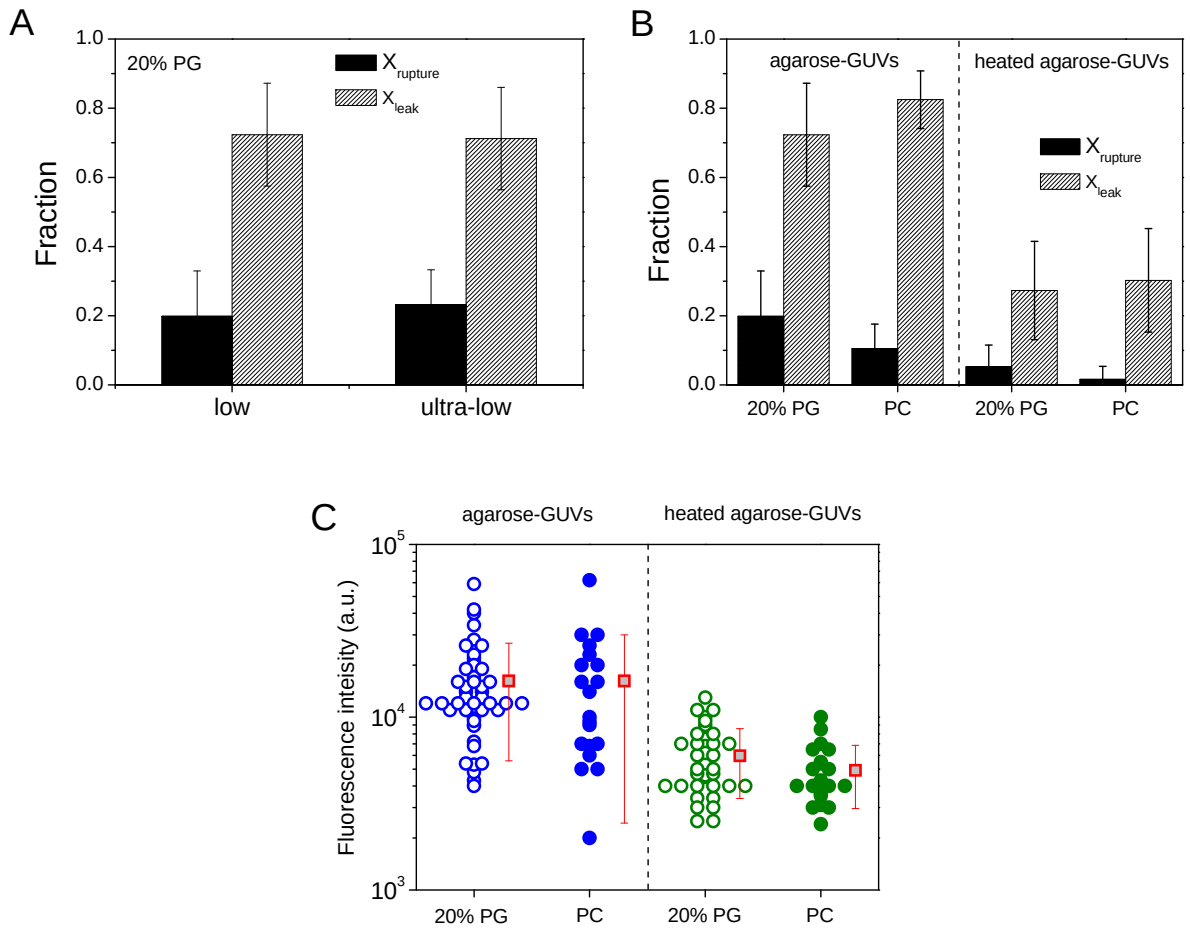


**Figure S4.** The behavior of agarose-GUVs is independent of agarose type and membrane composition. A) Comparison of $X_{rupture}$ and $X_{leak}$ for low and ultra-low gelling temperature agarose-GUVs (POPC:POPG 8:2). B) Comparison of $X_{rupture}$ and $X_{leak}$ data obtained with pure POPC and POPC:POPG 8:2 (low gelling temperature) agarose-GUVs (before and after heating). C) Agarose fluorescence intensity inside vesicles before (blue) and after (green) temperature treatment of (low gelling temperature) agarose-GUVs of pure POPC and POPC:POPG 8:2. Red squares represent mean values with standard deviations.

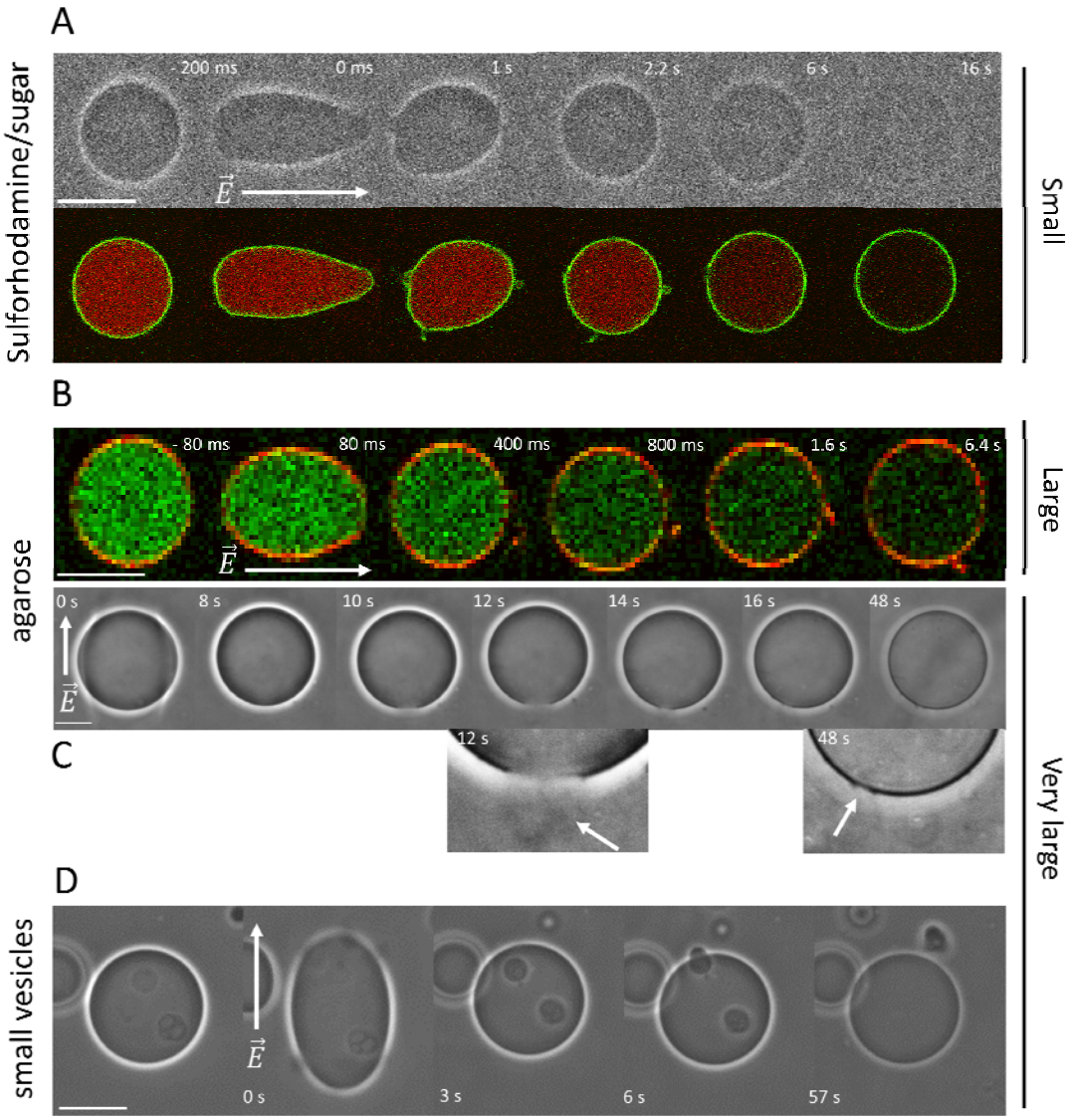


**Figure S5.** Materials of different sizes can permeate across the membrane as a result of post-pulse increased permeability. A: Mixing of sugars (upper row) and release of encapsulated sulforhodamine - 2.5 μM (lower row) are observed. Note that release of both sugars and fluorescent dye occurs simultaneously. B: Release of encapsulated fluorescent agarose. C: Release of agarose well after electroporation (first image) upon spontaneous macropore formation (~10 s). Released agarose stays in the region of the macropore, leading to imperfect pore closure and increased membrane permeability, with eventual loss of contrast. Inset shows contrast-enhanced sections of the snapshots: At 12 s, expulsion of the gel-like meshwork through the macropore and at 48 s, imperfect macropore closure, pointed by arrows. This sequence is shown in Movie 3 (supporting information). D: Expulsion of two encapsulated small vesicles well after electroporation (0 s). Membrane is labeled with DPPE-Rh in A and with DPPE-NBD in B. Membrane composition POPC:POPG 8:2. Arrows represent direction of the field. Differences in image quality are related to time acquisition. Bars: 50 μm.

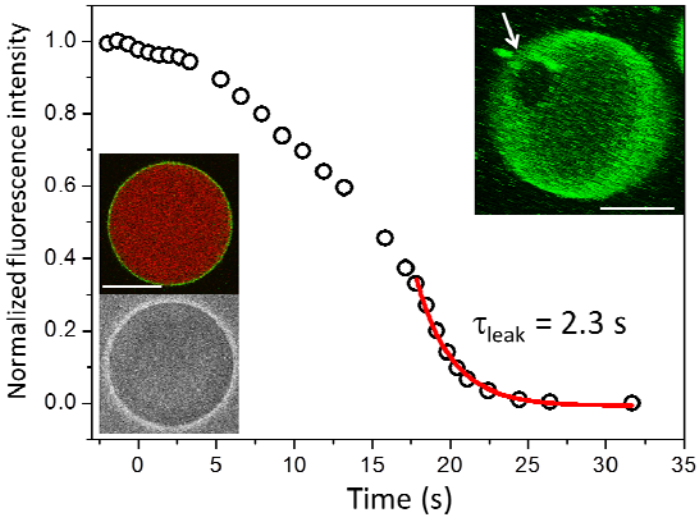


**Figure S6.** Fast release of encapsulated material due to formation of a stable macropore opened after the end of the pulse. Fluorescence from encapsulated sulforhodamine (2.5 μM) relative to medium fluorescence was measured over time from confocal images. Membrane contours detected by labeling with DPPE-NBD (0.5 mol%). The graph shows sulforhodamine leakage kinetics after pulse application. Leakage increases with time, indicating formation of more pores or increase in size of the present ones. The red curve is the exponential fit of the fastest decay, with its characteristic time $\tau_{leak}$. Note that all dye has leaked out. Left insets show the GUV before pulse application (confocal, upper, and phase contrast, lower, images). Right inset shows the 3D reconstruction image of this vesicle at ~1 min. Arrow shows the stable macropore. Membrane composition POPC:POPG 8:2. Bars: 20 μm.

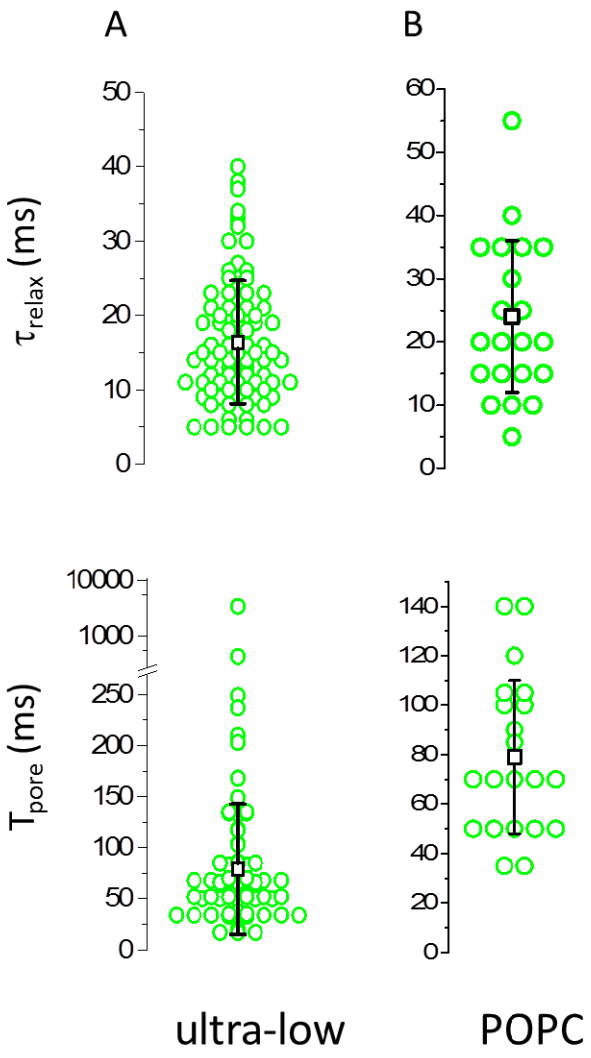


**Figure S7.** Hindered effects of agarose do not depend on membrane composition or on the type of polymer. In A, $\tau_{relax}$ and $T_{pore}$ values for pure POPC agarose-GUVs. In B, $\tau_{relax}$ and $T_{pore}$ values for ultralow gelling temperature agarose-GUVs made of POPC:POPG 8:2. Each point represents measurement on one vesicle. Black squares indicate mean values with standard deviations.

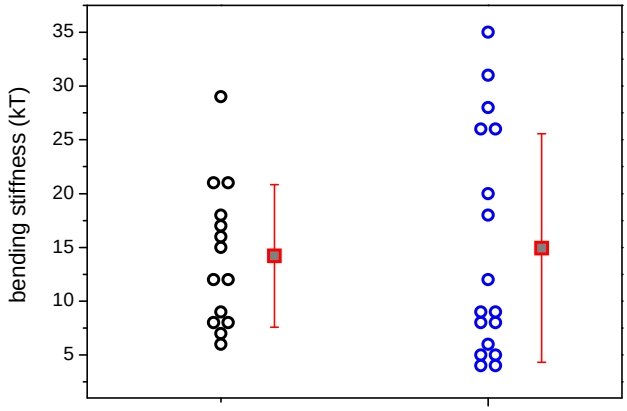


**Figure S8.** Values of bending rigidity measured at room temperature (~ 23 $^{o}$C). The data collected on agarose-GUVs shows a larger scatter, but no clear trend of increase or decrease of bending stiffness was observed, suggesting that encapsulated agarose does not significantly alters membrane elasticity. However, fluctuation analysis requires floppy vesicles, and therefore vesicles with high concentration of encapsulated agarose could not be probed.

## Movies

**Movie 1.** Movie sequence of Figure 2A (upper row, phase contrast) showing rupture and expulsion of the gel-like agarose meshwork. Agarose-GUV (diameter ~50 μm) composed of POPC:POPG 8:2 during application of a DC pulse of 3 kV/cm, 150 μs. Total time elapsed 7.1s.

**Movie 2.** Movie sequence of agarose-GUVs composed of POPC:POPG 8:2 observed with confocal microscopy during application of a DC pulse of 3 kV/cm, 150 μs. The membrane is labeled with 0.5 mol% DPPE-NBD (green) and the encapsulated dye is 2.5 μM sulforhodamine (red). Time elapsed is shown in seconds in the upper left corner and the scale bar is shown below. The video shows after-pulse permeability caused by the presence of encapsulated agarose.

**Movie 3.** Movie sequence of Figure S5C showing the leakage of encapsulated agarose through a macropore opened ~8s after application of a DC pulse of 3 kV/cm, 150 μs. Total time elapsed 5s.